

Characterizing Topological Excitations of a Long-Range Heisenberg Model with Trapped Ions

Stefan Birnkammer,^{1,2} Annabelle Bohrdt,^{1,2} Fabian Grusdt,^{3,1,2} and Michael Knap^{1,2}

¹*Department of Physics and Institute for Advanced Study,
Technical University of Munich, 85748 Garching, Germany*

²*Munich Center for Quantum Science and Technology (MCQST), Schellingstraße 4, 80799 München, Germany*

³*Department of Physics and Arnold Sommerfeld Center for Theoretical Physics (ASC),
Ludwig-Maximilians-Universität München, Theresienstr. 37, München D-80333, Germany*

(Dated: December 22, 2024)

Realizing and characterizing interacting topological phases in synthetic quantum systems is a formidable challenge. Here, we propose a Floquet protocol to realize the antiferromagnetic Heisenberg model with power-law decaying interactions. Based on analytical and numerical arguments, we show that this model features a quantum phase transition from a spin liquid to a valence bond solid that spontaneously breaks lattice translational symmetry and is reminiscent of the Majumdar-Ghosh state. The different phases can be probed dynamically by measuring the evolution of a fully dimerized state. We moreover introduce an interferometric protocol to characterize the topological excitations and the bulk topological invariants of our interacting many-body system.

Introduction.—Recent progress in realizing synthetic quantum systems has offered new opportunities for the experimental characterization and control of topological quantum phases. Topologically nontrivial band structures have been created by periodic driving [1–5], interaction-induced chiral propagation of excitations have been studied in the few-body limit of quantum Hall states [6, 7], and an interacting symmetry protected topological (SPT) phase has been realized in a Rydberg quantum simulator [8–10]. While first steps have been laid in realizing interacting topological phases, several challenges remain, in particular concerning the characterization and control of individual topological excitations.

Here, we propose the realization of a dimerized valence bond solid with topologically nontrivial excitations in a Heisenberg model with power-law interactions using trapped ions [11]. This phase arises due to frustration for interactions that are long-ranged enough and is adiabatically connected to the symmetry broken Majumdar-Ghosh phase of the Heisenberg model with nearest and next-to-nearest neighbor interactions [12–14]. When locally deforming this Hamiltonian to introduce bond alternating couplings, it realizes a Haldane SPT phase [15]. Our model therefore illustrates the interplay between spontaneous symmetry breaking and topological order. To realize the long-range Heisenberg model in a trapped-ion setting, we propose a simple Floquet protocol that consists of periodic globally-applied $\pi/2$ -pulses around different axes of the Bloch sphere, see Fig. 1 (a, b). Using analytical arguments and Matrix Product State (MPS) simulations, we establish the phase diagram, Fig. 1 (c), that can also be probed dynamically by studying the singlet evolution. Moreover, we propose an interferometric protocol to characterize the topological excitations and the bulk topological invariants of our interacting many-body system.

Model.—In the following, we investigate a long-range spin-1/2 Heisenberg chain with open boundaries

$$H_{\text{LR}}(\alpha) = \sum_{i < j} \frac{J}{|i-j|^\alpha} \left[\hat{S}_i^x \hat{S}_j^x + \hat{S}_i^y \hat{S}_j^y + \hat{S}_i^z \hat{S}_j^z \right], \quad (1)$$

where α is the power-law exponent of the long-range inter-

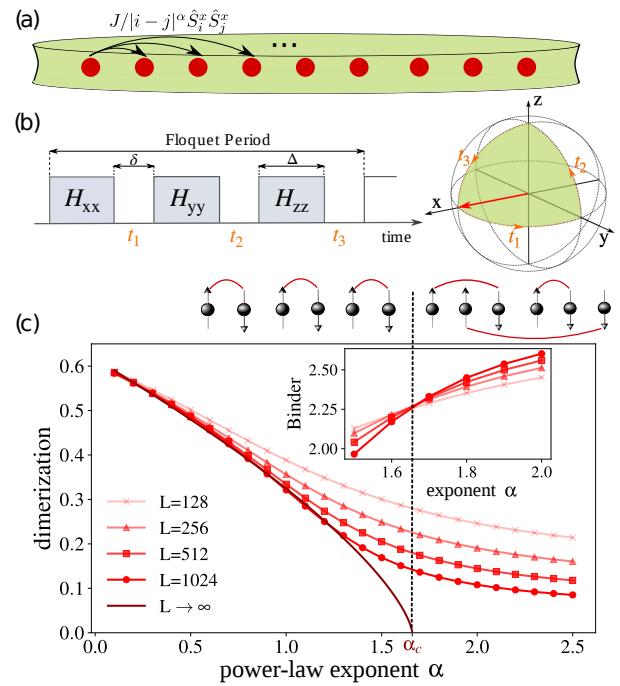


Figure 1. Illustration of the Floquet protocol and phase diagram.

(a) Interactions between ions in a linear Paul trap are of Ising type $H_{xx} = J/|i-j|^\alpha \hat{S}_i^x \hat{S}_j^x$. (b) Periodically applying global $\pi/2$ -pulses around different axes to encircle a surface area on the Bloch sphere (green), creates interactions along all three spin directions H_{xx} , H_{yy} , and H_{zz} . (c) The high frequency limit of such a protocol realizes a long-ranged Heisenberg model H_{LR} with effective $SU(2)$ symmetry. This model features a quantum phase transition from a dimerized to a liquid phase. Inset: Using a Binder cumulant analysis of the dimerization order parameter locates the transition at a critical power-law exponent of $\alpha_c \approx 1.66$.

actions and $J > 0$ their typical energy scale (for a spin-1 variant of the model see Ref. [16]). When considering only nearest and next-to-nearest neighbor couplings, $H_{\text{LR}}(\alpha)$ reduces to the Majumdar-Ghosh (MG) model [12, 13], which as a function of the ratio of the couplings exhibits a phase

transition from a liquid to a dimerized valence bond solid that breaks the translational invariance of the lattice [14]. In the following we generalize these observations to the long-range Heisenberg model H_{LR} .

Before we numerically study the detailed phase diagram of H_{LR} , we provide general considerations for the limiting cases of the power-law exponent α . For $\alpha \rightarrow \infty$ our model reduces to the conventional Heisenberg model with nearest-neighbor couplings whose ground state is a gapless spin liquid with power-law decaying antiferromagnetic correlations [17]. For $\alpha \rightarrow 0$, each spin interacts with all the other spins and hence $H_{\text{LR}}(\alpha \rightarrow 0) = \frac{J}{2} \vec{S} \cdot \vec{S}$, where \vec{S} represents a collective spin with extensive magnitude. The states with minimal energy of this Hamiltonian correspond to spin-0 states, as suggested by Marshall's theorem [18, 19]. For the strict limit of $\alpha = 0$ a highly degenerate ground state manifold can be constructed by considering arbitrary singlet pairings of the original spin-1/2 degrees of freedom. This degeneracy is, however, lifted as soon as we consider small but finite α . In that case, it is energetically favorable to form $L/2$ singlets on neighboring sites as in the Majumdar-Ghosh state

$$|\text{MG}\rangle = \prod_i^{L/2} (|\uparrow\rangle_{2i} |\downarrow\rangle_{2i+1} - |\downarrow\rangle_{2i} |\uparrow\rangle_{2i+1}) / \sqrt{2}. \quad (2)$$

As a consequence the ground state breaks translational symmetry for small α , cf. supplementary material [20]. Due to the different behavior of the ground states in the two limits, a phase transition is expected at some critical α_c .

To estimate the critical value α_c , we perform Density-Matrix Renormalization Group (DMRG) simulations [21] and compute the dimerization order parameter

$$d_i = \vec{S}_{2i} \cdot (\vec{S}_{2i+1} - \vec{S}_{2i-1}). \quad (3)$$

as a function of α and for different system sizes L , see Fig. 1 (c). In agreement with our previous arguments, an analysis of the Binder cumulant $\langle d^4 \rangle / \langle d^2 \rangle^2$, that is expected to be scale-independent at criticality [22, 23], suggests a quantum phase transition from a dimerized phase to a liquid at $\alpha_c \approx 1.66$ (inset). Precisely extracting the critical point is a formidable challenge for Majumdar-Ghosh type models, as renormalization group studies uncover marginal couplings that require the study of exponentially large chains as the critical regime is approached [14, 24, 25]. In our numerical studies we represent the Hamiltonian as a Matrix Product Operator, in which we approximate the power-law coupling by a sum of exponentials [26, 27]. To obtain a feasible approximation even for very large distances between interacting spins, we have to take sufficiently many exponentials into account, which limits our maximal system size to $L \lesssim 10^3$. We emphasize, however, that for the following discussions the precise location of the phase transition is not crucial.

Floquet Protocol.—Collective vibrations of an ion crystal mediate long-range Ising interactions $H_{xx} = \sum_{i < j} J/|i - j|^\alpha S_i^x S_j^x$ [28, 29]. Previous works suggested to use multiple

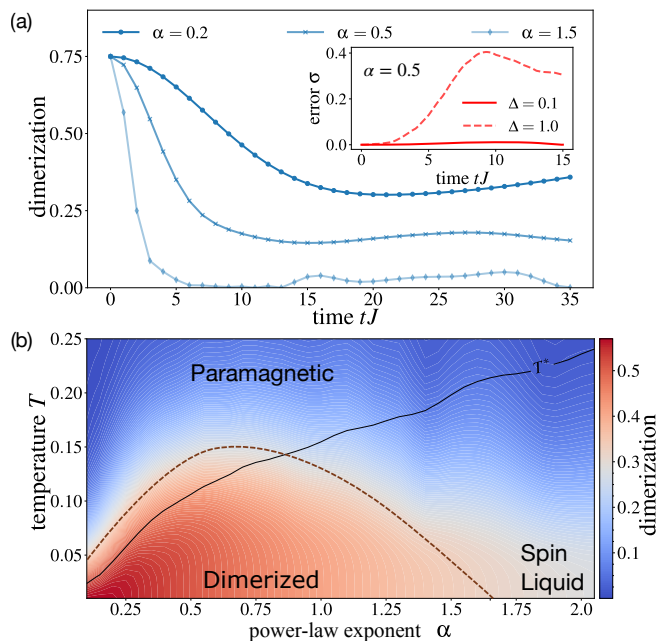


Figure 2. **Dynamical phase diagram.** (a) Evolution of the dimerization d under the Floquet dynamics for an initial $|\text{MG}\rangle$ -state of singlets. The evolution is governed by $H_{\text{LR}}(\alpha)$ for $\alpha \in \{0.2, 0.5, 1.5\}$ and a chain of 64 sites. Inset: We illustrate the relative deviation $\sigma \equiv |(d_{\Delta \rightarrow 0} - d_{\Delta}) / d_{\Delta \rightarrow 0}|$ of the Floquet protocol from the exact evolution for different values of Δ and $\alpha = 0.5$. (b) Thermal phase diagram for $H_{\text{LR}}(\alpha)$ including the effective temperature T^* of our system quenched from the $|\text{MG}\rangle$ -state (solid line) and a schematic of the phase boundary between the dimerized valence bond solid and the translational invariant phases (dashed dome).

phonon branches [30] and quasi-periodic driving [31] to realize Heisenberg type interactions, or have employed digital simulation schemes [32]. Here, we suggest a simple way to realize $SU(2)$ invariant Heisenberg interactions, by periodically applying global $\pi/2$ -pulses around different axes to encircle a surface of the Bloch sphere, as sketched in Fig. 1 (b). We can safely assume that the duration δ of the $\pi/2$ -pulses for a trapped ion setting is much shorter than the waiting time Δ between the pulses, leading to an effective driving period of $\approx 3\Delta$. This way the many-body state rotates periodically from the x over y to z direction. These unitary transformations can also be interpreted to act on the Hamiltonian instead of the many-body state, leading to an effective time evolution with alternating H_{xx} , H_{yy} , and H_{zz} Ising couplings. Provided the rate Δ^{-1} is fast compared to the typical interaction strength J , a high-frequency expansion [33] for the effective periodic drive can be computed, which to leading order yields the $SU(2)$ invariant Hamiltonian (1).

Singlet evolution.—As a direct application of the Floquet protocol, we compute the time evolution of the long-range Heisenberg model $H_{\text{LR}}(\alpha)$ for an initial singlet state $|\text{MG}\rangle$ using the time-dependent variational principle for MPS [21, 34–36]. For quenches to small α , we find that the dimerization remains finite at long times, whereas it quickly decays to zero

for quenches to large α , see Fig. 2 (a). To compare the discrete Floquet evolution with the exact dynamics of $H_{LR}(\alpha)$, we introduce the relative deviation $\sigma \equiv |(d_{\Delta \rightarrow 0} - d_{\Delta})/d_{\Delta \rightarrow 0}|$, shown in the inset of Fig. 2 (a) for $\alpha = 0.5$. We find that the Floquet protocol accurately describes the $SU(2)$ invariant Heisenberg evolution for $\Delta = 0.1J$ (depending on α , larger values of $\Delta \sim J$ can be safely reached [20]).

The energy density of the dimerized initial state is $\langle \text{MG} | H_{LR}(\alpha) | \text{MG} \rangle / L = -0.375$ independent of α , which is larger than the ground-state energy density of $H_{LR}(\alpha)$. Hence, the quench deposits an extensive amount of energy into the system. According to the eigenstate thermalization hypothesis [37–39], which is expected to hold for generic interacting systems as this, a subsystem should thermalize to an effective temperature T^* , that is consistent with the energy density deposited in the system. The effective temperature can then be evaluated self-consistently from the condition $\langle \text{MG} | H_{LR}(\alpha) | \text{MG} \rangle = \text{tr}[H_{LR}(\alpha) e^{-H_{LR}(\alpha)/T^*} / \mathcal{Z}]$ where \mathcal{Z} is the partition sum. We approximate the thermal expectation value using the typicality approach [40] and evolve 80 random initial states in imaginary time using exact diagonalization on 16 spins. With that approach we solve the self-consistent equation for the effective temperature T^* as a function of α . The results are shown in Fig. 2 (b), solid line, along with the temperature dependent dimerization, heat map. The effective temperature increases with α as the ground state deviates increasingly from the dimerized $|\text{MG}\rangle$ -state and hence an increasing amount of energy is deposited in the system. From this dynamical phase diagram, we find that for $\alpha \lesssim 1$ the effective temperature is low enough such that a finite dimerization is supported in the steady state of the system, whereas it should decay to zero for $\alpha \gtrsim 1$, consistent with our observations on the full time evolution in Fig. 2 (a).

Measuring the Zak phase.—Starting from the $|\text{MG}\rangle$ -state, a state close to the ground state of $H_{LR}(\alpha)$ can be prepared by adiabatically tuning α as long as the system remains in the dimerized phase. We will now present a protocol to measure a topological order parameter of such a state. Following Refs. [41, 42], we introduce the $SU(2)$ -transformation

$$\Phi : \vec{S}_i \cdot \vec{S}_j \mapsto \hat{S}_i^z \hat{S}_j^z + \frac{1}{2} (e^{i\varphi} \hat{S}_i^+ \hat{S}_j^- + \text{h.c.}), \quad (4)$$

where φ is a compact variable in the interval $[0, 2\pi]$. The $SU(2)$ -transformation is designed such that it affects only couplings crossing the ℓ -th bond between sites ℓ and $\ell + 1$, which separates our system into a left S_L and a right S_R part. All interactions within one subsystem remain unchanged. As a consequence we obtain for every choice of the bond ℓ a new family of Hamiltonians $H_{LR}(\alpha; \varphi)$ parametrized by $\varphi \in [0, 2\pi]$.

A key for obtaining a quantized topological order parameter is that the chosen parametrization retains the time-reversal symmetry of $H_{LR}(\alpha; \varphi)$ [41]. Tuning φ continuously through the interval $[0, 2\pi]$, describes a closed loop C_ℓ within the set

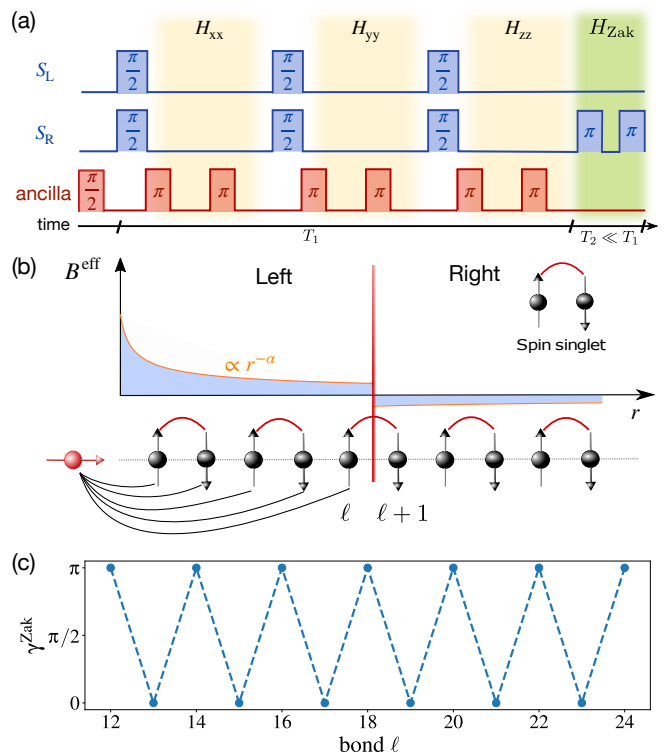


Figure 3. Interferometric protocol to measure many-body Zak phases. (a) A $\pi/2$ -pulse initializes the ancilla qubit (red) before performing the Floquet protocol on the system (blue), which we divide into a left S_L and a right S_R part. During the system evolution the accumulated phase of the ancilla is canceled by consecutive π pulses. As a last step of the Floquet step, a π -pulse is applied to the right part of the system, which induces a sign change in the effective interaction between the ancilla and S_R , which is then reverted again at the end of the step. (b) The effective field B^{eff} acting on the system during the last step of the protocol has a sign change at the bond where we measure γ_ℓ^{Zak} . (c) Performing measurements according to this protocol for different ℓ yields alternating Zak phases γ_ℓ^{Zak} of 0 or π . Data is evaluated for a system of 32 sites and $\alpha = 0.2$.

of Hamiltonians. This allows us to introduce the Zak phase

$$\gamma_\ell^{\text{Zak}} = \oint_{C_\ell} d\varphi \langle \psi(\varphi) | i\partial_\varphi | \psi(\varphi) \rangle, \quad (5)$$

where $|\psi(\varphi)\rangle$ is the ground state of $H_{LR}(\alpha; \varphi)$. The Zak phase is well defined, provided the corresponding path C_ℓ is followed adiabatically, which can be ensured because the dimerized phase is gapped, see supplementary material [20]. In order to gain some intuition about the Zak phase, we first apply the $SU(2)$ -transformation to the fully dimerized $|\text{MG}\rangle$ -state. When the bond ℓ lies within a singlet, the transformation gives $(|\uparrow\downarrow\rangle - e^{i\varphi} |\downarrow\uparrow\rangle) / \sqrt{2}$. Evaluating Eq. (5) for this particular case reveals a Zak-phase of π [43, 44], while it is zero when the bond ℓ lies between two singlets. For the $|\text{MG}\rangle$ -state and thus also for the adiabatically connected ordered ground states of H_{LR} we consequently expect to find a Zak phase alternating between values of 0 or π when traversing the bond ℓ through the system.

Before we numerically compute the Zak phase of the dimerized state, we introduce a protocol to experimentally measure it in a trapped ion setting. Let us first gain some intuition: To realize a transformation similarly to (4), we can use an effective (in general time-dependent) magnetic field acting on the spins of $H_{\text{LR}}(\alpha)$, that is proportional to a step function with the step being located at bond ℓ : $\sum_i B_i^{\text{eff}}(t) \hat{S}_i^z$. Using the Peierls substitution, the magnetic field can be absorbed into Hamiltonian as $H_{\text{LR}}(\alpha; \varphi(t)) = \sum_{i < j} J/|i-j|^\alpha [S_i^z S_j^z + \frac{1}{2}(e^{i\varphi_{ij}(t)} S_i^+ S_j^- + \text{h.c.})]$, where $\varphi_{ij}(t) \equiv \int_0^t dt' [B_j^{\text{eff}}(t') - B_i^{\text{eff}}(t')]$. A phase is only picked up, when bond ℓ is crossed as B_i^{eff} is assumed to be constant except across bond ℓ . The time t can then be chosen such that the phase φ is adiabatically tuned from 0 to 2π . The Zak phase can then be measured using a Ramsey sequence to cancel dynamical phases [45–47].

In order to implement this approach in a chain of ions, we identify the left-most ion as an ancilla qubit τ^z that has the conventional power-law coupling to the other spins of the chain $\sum_i J/|i|^\alpha \tau^z \hat{S}_i^z \equiv \sum_i B_i^{\text{eff}} \hat{S}_i^z$. The protocol then consists of the following steps, see Fig. 3 (a) for an illustration: (i) Initialize the ancilla qubit in a superposition state by applying a $\pi/2$ -rotation. This leads to an opposite sign in B^{eff} for the two ancilla states and in turn allows for a cancellation of the dynamical phase. (ii) Perform global $\pi/2$ -rotations on the system around different axes, as discussed in Fig. 1 (b), to realize the long-range Heisenberg dynamics. During that time perform equally spaced π -rotations on the ancilla qubit to cancel the phase accumulation. (iii) After a Floquet period, apply a π -rotation only on the right part of the system to create an effective field B_i^{eff} between the ancilla and the system with a kink at bond ℓ , see Fig. 3 (b). Accumulate phase on the ancilla for a period that is short compared to the evolution time to maintain adiabaticity. Apply another π -rotation to restore the couplings within the system. Steps (ii) and (iii) are then repeated until φ covers the whole interval $[0, 2\pi]$. (iv) Measure the phase of the ancilla by applying a final $\pi/2$ -rotation. This phase corresponds to the Zak phase of Eq. (5) at bond ℓ .

In the proposed experimental protocol, the effective field has the required jump at bond ℓ , but additionally is slowly varying across the other bonds. We will now demonstrate the robustness of this protocol by numerically evaluating the Zak phase in Eq. (5). Using DMRG we compute the ground state for 20 discretized steps along \mathcal{C}_ℓ for a system of 32 sites and $\alpha = 0.2$, see Fig. 3 (c), which confirms that the Zak phase is alternating between 0 and π as indicative for a dimerized state. As a gauge choice we fixed the phase of initial states to $\varphi = 0$. We also confirm the adiabaticity of the computation by calculating the product of projectors into the ground state $\mathcal{P}(\varphi) = |\psi(\varphi)\rangle \langle \psi(\varphi)|$ during each step of the protocol, which is given by $\Gamma_N = \prod_{\varphi_n \in [0, 2\pi]} \langle \psi(\varphi_{n+1}) | \psi(\varphi_n) \rangle$. We numerically find that $|\Gamma_N|$ attains values between 0.75 to 1, confirming the adiabaticity of the discretized contours.

Topological excitations.—In order to characterize the topological excitations of the dimerized phase, we now consider a chain with an odd number of sites. In this case, singlets cannot

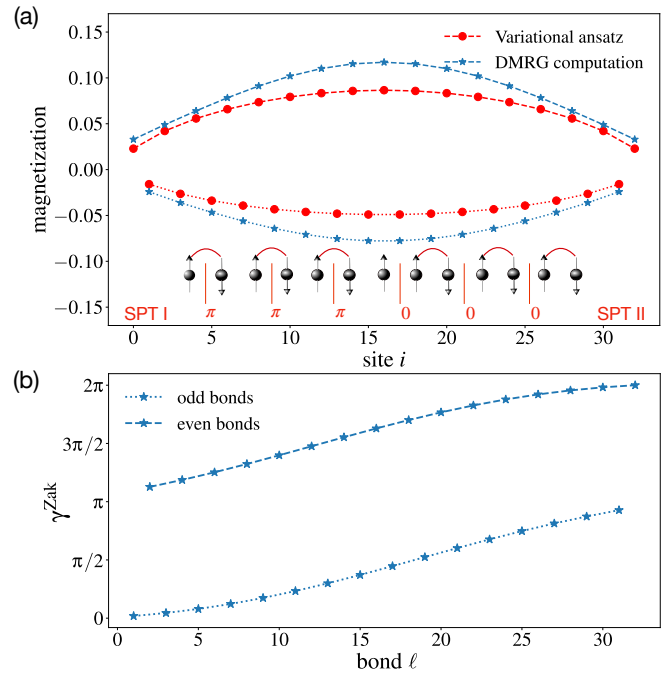


Figure 4. **Topological excitations.** (a) Local magnetization for a spin in a lattice of 33 sites and $\alpha = 0.2$. We compare the DMRG result with a variational Ansatz delocalizing a single spinon. (b) This bulk excitation swaps the Zak phase of even and odd bonds as the bond ℓ moves across the system.

fully cover the chain, and hence an unpaired spin-1/2 (spinon) excitation is always present. Due to prominent examples such as the AKLT model [48] we are used to the existence of spin-1/2 states in interacting topological phases. These degenerate modes provide a clear signature for topological order and are typically localized at the edges of the system. In contrast to the usual edge modes, a measurement of the magnetization for H_{LR} indicates that the excitation is delocalized over the entire lattice, see Fig. 4 (a). In order to obtain an analytical understanding, we introduce a variational state $|\psi_{\text{var}}(q)\rangle = \frac{1}{\mathcal{N}(q)} \sum_{l=0}^{(L-1)/2} [\sin(q(2l+1)) + \sin(q(L-2l))] |2l\rangle$, where $|2l\rangle = \prod_{i=0}^{l-1} |s\rangle_{2i, 2i+1} \otimes |\uparrow\rangle_{2l} \otimes \prod_{i=l+1}^{(L-1)/2} |s\rangle_{2i-1, 2i}$ and $|s\rangle = (|\uparrow\downarrow\rangle - |\downarrow\uparrow\rangle)/\sqrt{2}$. This state describes a delocalized spinon at position $2l$ separating two $|MG\rangle$ -states with singlets on even and odd bonds, respectively. The spinon hence represents a defect in the topological order; inset of Fig. 4 (a). Variationally optimizing the ground state energy with our Ansatz yields $q = \frac{\pi L}{2(L+1)}$, which is consistent with the oscillatory magnetization pattern in Fig. 4 (a).

We also characterize the Zak phase for this state. For odd sites, the dimerized ground state of the system is two-fold degenerate due to the $SU(2)$ symmetry of our model and hence we cannot construct an adiabatic path \mathcal{C}_ℓ . To lift the degeneracy, we apply a weak local magnetic field in the center of the system, which introduces a small gap. This magnetic field breaks time reversal symmetry. From the arguments of Hat-

sugai [41, 42] it then follows that the Zak phase is not quantized in general. As a consequence, we expect a monotonous change in the Zak phase as we traverse the system from left to right which can be interpreted as a domain wall separating two distinct topological phases. Our numerical results are indeed consistent with this picture, see Fig. 4 (b) and also show that the Zak phase of even and odd bonds differ by $\sim \pi$ as advocated by the domain wall picture.

Outlook.—Our studies uncovered that the Heisenberg model with long-range antiferromagnetic interactions exhibits a phase transition from a liquid phase to a dimerized valence bond solid that spontaneously breaks the lattice translational invariance. We propose Floquet protocols for trapped ions to realize this interacting model and to characterize the nature of the delocalized topological excitations as well as the bulk topological invariants.

For future studies, it would be interesting to introduce an easy-axis anisotropy by adjusting the Floquet periods between the $\pi/2$ -pulses to realize a deconfined quantum critical point between a dimerized and a Néel ordered phase in our one-dimensional model [49, 50] or to explicitly break the translational symmetry by introducing bond-alternating couplings to realize a Haldane SPT phase with localized edge states [15]. A future challenge is to develop protocols that realize interacting higher-dimensional topological many-body states with synthetic quantum matter that are characterized by topological entanglement entropy and fractional excitations [51].

Acknowledgements.—We thank R. Blatt, E. Demler, Ch. Maier, F. Pollmann, and R. Verresen for insightful discussions. We acknowledge support from the Technical University of Munich - Institute for Advanced Study, funded by the German Excellence Initiative and the European Union FP7 under grant agreement 291763, the Deutsche Forschungsgemeinschaft (DFG, German Research Foundation) under Germanys Excellence Strategy–EXC–2111–390814868, TRR80 and DFG grant No. KN1254/2-1, No. KN1254/1-2, Research Unit FOR 2414 under project number 277974659, and from the European Research Council (ERC) under the European Unions Horizon 2020 research and innovation programme (grant agreement No. 851161).

Supplemental Materials

All-to-all Interactions.—Here, we discuss the limiting case $\alpha = 0$ of H_{LR} , in which our one-dimensional model describes a cluster of spins forming one self-interacting spin of extensive magnitude \vec{S} :

$$\begin{aligned} \hat{H}_{\text{LR}}(\alpha = 0) &= J \sum_{i < j} \vec{S}_i \cdot \vec{S}_j \\ &= \frac{J}{2} \sum_{i,j} \vec{S}_i \cdot \vec{S}_j - \frac{J}{2} \sum_i \vec{S}_i^2 \\ &= \frac{J}{2} \vec{S} \cdot \vec{S} - \frac{3J}{8} L. \end{aligned} \quad (6)$$

To arrive at the final expression we introduced $\vec{S} \equiv \sum_i \vec{S}_i$ and made use of the identity for amplitudes of spin operators $\vec{S} \cdot \vec{S} = s(s+1)$.

The energy spectrum of the model can now be completely determined by representation theory of the group $SU(2)$. To this end, we look at all possible irreducible representations arising from a product of L spin-1/2 degrees of freedom. We will first assume an even number of spins L . The arising representations are given by

$$\bigotimes_{i=1}^L \mathbf{D}^{1/2} = \bigoplus_{j=0}^{L/2} \bigoplus_{n=1}^{N_j} \mathbf{D}^j, \quad (7)$$

where we denoted an irreducible representation of spin j as \mathbf{D}^j following the notation of Cornwell and Buck [52]. Expression (7) indicates that we have N_j distinct irreducible $SU(2)$ -representations \mathbf{D}^j , where j ranges up to total spin $L/2$. The energy E_j corresponding to each spin representation \mathbf{D}^j is according to Hamiltonian (6) given as

$$E_j = \frac{J}{2} j(j+1) - \text{const}. \quad (8)$$

The ground states of the theory are hence given by all singlet representations arising from the product of L spins, which is also conjectured by the theorem of Marshall for quantum antiferromagnetic Heisenberg models [18, 19]. Next we determine the degeneracies of energy levels, which are directly related to the set $\{N_j\}$, because we find precisely $N_j(2j+1)$ states of energy E_j . First, we note that these degeneracies carry a dependence on the system size L . This is required to ensure an exponential growth of the Hilbert space as we extend our system with additional spins. Although also higher spin representations will be made accessible by additional spins, latter only cause a linear increase in the dimension of the Hilbert space.

We can now use the L -dependence to determine recursive relations for every $N_j(L)$ respectively. For this purpose we will first look at a small system and then generalize our observations to arbitrary system sizes. We start by adding an additional spin doublet to a system of only $L = 2$ spins. The corresponding decomposition into irreducible representations \mathbf{D}^j is given by

$$\begin{aligned} (\mathbf{D}^{1/2} \otimes \mathbf{D}^{1/2}) \otimes (\mathbf{D}^{1/2} \otimes \mathbf{D}^{1/2}) \\ &= (\mathbf{D}^0 \oplus \mathbf{D}^1) \otimes (\mathbf{D}^0 \oplus \mathbf{D}^1) \\ &= (\mathbf{D}^0 \oplus \mathbf{D}^1) \oplus (\mathbf{D}^1 \oplus \mathbf{D}^0 \oplus \mathbf{D}^1 \oplus \mathbf{D}^2) \\ &= \mathbf{D}^0 \oplus \mathbf{D}^0 \oplus \mathbf{D}^1 \oplus \mathbf{D}^1 \oplus \mathbf{D}^1 \oplus \mathbf{D}^2. \end{aligned} \quad (9)$$

Here, we used distributivity as well as the Clebsch-Gordan series for products of two irreducible $SU(2)$ -representations.

We notice that the added singlet representation reproduces all given representations of the previous system. The triplet contained in the added spin doublet will produce three new representations for every previous one. For the example of (9) this concretely increases N_0 by 1, N_1 by 2 and N_2 by 1. If we

look at the situation, given in (9), on more general grounds we recognize that \mathbf{D}^0 can only result from a product of two singlets or two triplets. All other spin representations can, however, be generated from previous ones in four different ways. The spin can on the one hand be kept constant by an product with \mathbf{D}^0 or \mathbf{D}^1 . On the other hand it can be increased or decreased by 1 using the product with \mathbf{D}^1 . This behavior is summed up to the following recursive sequence for the set of $\{N_j(L)\}$.

$$\begin{aligned}
 N_0(L+2) &= N_0(L) + N_1(L) \\
 N_1(L+2) &= N_0(L) + 2N_1(L) + N_2(L) \\
 N_2(L+2) &= N_1(L) + 2N_2(L) + N_3(L) \\
 &\vdots \\
 N_n(L+2) &= N_{n-1}(L) + 2N_n(L) + N_{n+1}(L)
 \end{aligned}
 \tag{10}$$

This set of equations can be implemented and solved symbolically, determining the entire spectrum of $H_{\text{LR}}(\alpha = 0)$.

After investigating the exact limit $\alpha = 0$ let us now discuss the implications for small but positive α . Recalling Marshall's theorem [18] we still expect to find an overall singlet as the ground state of our system. On the contrary to the previous discussion we do, however, not expect to find a degeneracy in the ground state. High degeneracies are expected for the case $\alpha = 0$ as interactions do not introduce a definite order in the system and we can reorder the spins in all possible ways. This is no longer possible for $\alpha > 0$, where the decaying interactions favor nearby singlets. For this reason we expect the ground state to exhibit a large overlap with $|\text{MG}\rangle$, defined in the main text and possesses a finite dimerization d .

Energy Gaps of Ordered Phase.—After investigating the ground state of the system, we can use our previous results to discuss also excited states and especially the existence of finite energy gaps in the dimerized phase. The latter are especially important for an adiabatic implementation of our protocol to measure geometric Zak phases.

For the case of even L and very small α we expect to find an overall spin-singlet even for the first excited states, since all spin-0 configurations only receive small corrections increasing with α compared to the degenerate case of $\alpha = 0$. The gaps of all higher spin representations are, however, still determined up to a factor by (8) to be finite and $\mathcal{O}(J)$. Even though an analytical calculation of the gap is challenging, intuition can be gained from mapping our long-ranged spin model H_{LR} to a Non-Linear Sigma model (NLSM) with a topological term [15, 31, 53]. A renormalization analysis indicates that such a system either flows to a gapless fixed point of a $SU(2)_1$ Wess-Zumino-Witten conformal field theory or approaches a gapped fixed point. These limits are related to the disordered gapless and the gapped ordered phase of our model. We test this conjecture numerically in Fig. 5. For small α our finite size analysis supports a converged energy gap above the ground state. As the critical point $\alpha_c \approx 1.66$ is approached, the required system sizes to observe an onset of saturation increases.

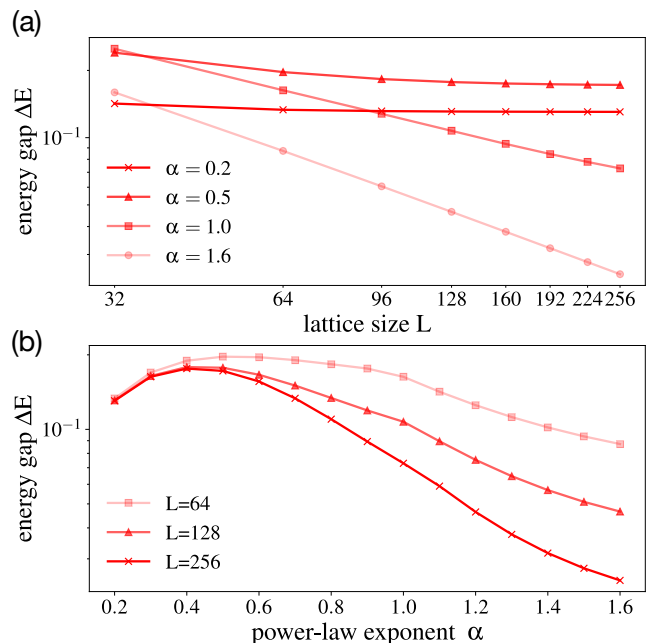


Figure 5. **Energy Gaps.** Energy gap ΔE above the ground state (a) as a function of the lattice size L and (b) as a function of α .

A short remark should be addressed to the case of odd-numbered system sizes. Whereas finite energy gaps above the ground state were shown to exist naturally in the ordered phase for systems with an even number of sites, the situation is different for odd L . Although the previous arguments for a gap between the various spin representations apply in the same way for odd L , they also conserve the degeneracy within each representation. This fact directly results from the $SU(2)$ symmetry of H_{LR} . Contrary to the spin singlet for even lattice sizes transforming trivially under application of group generators from $su(2)$, the ground state spin-1/2-representation for odd L allows a mixing of both polarization directions of the spinon excitation. The ground state degeneracy will hence remain two-fold unless we break the underlying $SU(2)$ symmetry. This can for instance be achieved with a small but finite local magnetic field, causing an energy splitting within each spin representation and creating a finite gap above the ground state.

Convergence of the Floquet Protocol.—We numerically study the convergence of the driven Hamiltonian to its high-frequency limit H_{LR} . To this end, we investigate the time-evolution of a maximally dimerized $|\text{MG}\rangle$ -state for both cases. The numerical results are shown in Fig. 6 for Floquet step durations of $\Delta \in \{0.1, 1.0\}J$ and $\alpha \in \{0.1, 1, 2\}$. We find fast convergence to the evolution governed by H_{LR} even for comparatively low driving frequencies ($\Delta = 1.0J$) both deep in the dimerized phase ($\alpha = 0.1$) and in the fluid phase ($\alpha = 2.0$), whereas closer to the critical regime shorter periods are required. All in all, the effective Floquet Hamiltonian approximates H_{LR} reasonably well already for not-too-high driving frequencies which simplifies an experimental realiza-

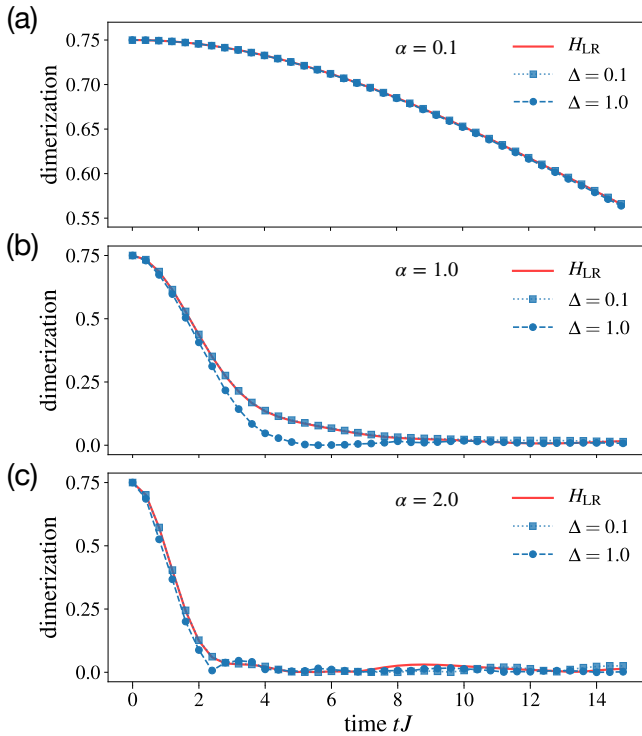


Figure 6. **Convergence of the Floquet Protocol.** The convergence of the Floquet Hamiltonian towards its infinite-frequency limit H_{LR} is examined by comparing time-evolution of $|\text{MG}\rangle$ -states in different regions of the phase diagram: (a) $\alpha = 0.1$, (b) $\alpha = 1.0$, and (c) $\alpha = 2.0$ for different values of the Floquet period Δ .

tion.

[1] M. Aidelsburger, M. Atala, M. Lohse, J. T. Barreiro, B. Paredes, and I. Bloch, “Realization of the hofstadter hamiltonian with ultracold atoms in optical lattices,” *Physical Review Letters* **111**, 185301 (2013).

[2] Hirokazu Miyake, Georgios A. Siviloglou, Colin J. Kennedy, William Cody Burton, and Wolfgang Ketterle, “Publisher’s note: Realizing the harper hamiltonian with laser-assisted tunneling in optical lattices [phys. rev. lett.111, 185302 (2013)],” *Physical Review Letters* **111**, 199903 (2013).

[3] Gregor Jotzu, Michael Messer, Rémi Desbuquois, Martin Lebrat, Thomas Uehlinger, Daniel Greif, and Tilman Esslinger, “Experimental realization of the topological haldane model with ultracold fermions,” *Nature* **515**, 237–240 (2014).

[4] N. Flaschner, B. S. Rem, M. Tarnowski, D. Vogel, D.-S. Luhmann, K. Sengstock, and C. Weitenberg, “Experimental reconstruction of the berry curvature in a floquet bloch band,” *Science* **352**, 1091–1094 (2016).

[5] Karen Wintersperger, Christoph Braun, F. Nur Ünal, André Eckardt, Marco Di Liberto, Nathan Goldman, Immanuel Bloch, and Monika Aidelsburger, “Realization of an anomalous floquet topological system with ultracold atoms,” *Nat. Physics* **16**, 1058–1063 (2020).

[6] M. Eric Tai, Alexander Lukin, Matthew Rispoli, Robert Schittko, Tim Menke, Dan Borgnia, Philipp M. Preiss, Fabian

Grusdt, Adam M. Kaufman, and Markus Greiner, “Microscopy of the interacting harper–hofstadter model in the two-body limit,” *Nature* **546**, 519–523 (2017).

[7] P. Roushan, C. Neill, A. Megrant, Y. Chen, R. Babbush, R. Barends, B. Campbell, Z. Chen, B. Chiaro, A. Dunsworth, A. Fowler, E. Jeffrey, J. Kelly, E. Lucero, J. Mutus, P. J. J. O’Malley, M. Neeley, C. Quintana, D. Sank, A. Vainsencher, J. Wenner, T. White, E. Kapit, H. Neven, and J. Martinis, “Chiral ground-state currents of interacting photons in a synthetic magnetic field,” *Nature Physics* **13**, 146–151 (2017).

[8] Zheng-Cheng Gu and Xiao-Gang Wen, “Tensor-entanglement-filtering renormalization approach and symmetry-protected topological order,” *Phys. Rev. B* **80**, 155131 (2009).

[9] Frank Pollmann, Erez Berg, Ari M. Turner, and Masaki Oshikawa, “Symmetry protection of topological phases in one-dimensional quantum spin systems,” *Phys. Rev. B* **85**, 075125 (2012).

[10] Sylvain de Léséleuc, Vincent Lienhard, Pascal Scholl, Daniel Barredo, Sebastian Weber, Nicolai Lang, Hans Peter Büchler, Thierry Lahaye, and Antoine Browaeys, “Observation of a symmetry-protected topological phase of interacting bosons with rydberg atoms,” *Science* **365**, 775–780 (2019).

[11] R. Blatt and C. F. Roos, “Quantum simulations with trapped ions,” *Nat. Physics* **8**, 277–284 (2012).

[12] Chanchal K. Majumdar and Dipan K. Ghosh, “On next-nearest-neighbor interaction in linear chain. i,” *J. Math. Phys.* **10**, 1388–1398 (1969).

[13] Chanchal K. Majumdar and Dipan K. Ghosh, “On next-nearest-neighbor interaction in linear chain. ii,” *J. Math. Phys.* **10**, 1399–1402 (1969).

[14] Steven R. White and Ian Affleck, “Dimerization and incommensurate spiral spin correlations in the zigzag spin chain: Analogies to the kondo lattice,” *Physical Review B* **54**, 9862–9869 (1996).

[15] F. D. M. Haldane, “Continuum dynamics of the 1-d heisenberg antiferromagnet: Identification with the o(3) nonlinear sigma model,” *Physics Letters A* **93**, 464–468 (1983).

[16] Z.-X. Gong, M. F. Maghrebi, A. Hu, M. L. Wall, M. Foss-Feig, and A. V. Gorshkov, “Topological phases with long-range interactions,” *Phys. Rev. B* **93**, 041102 (2016).

[17] Thierry Giamarchi, *Quantum Physics in One Dimension* (Oxford University Press, Oxford, 2004).

[18] W. Marshall, “Antiferromagnetism,” *Proceedings of the Royal Society of London Series A* **232**, 48–68 (1955).

[19] Assa Auerbach, *Interacting electrons and quantum magnetism* (Springer, 1994).

[20] See supplementary material for details.

[21] Johannes Hauschild and Frank Pollmann, “Efficient numerical simulations with Tensor Networks: Tensor Network Python (TeNPy),” *SciPost Phys. Lect. Notes* , 5 (2018).

[22] Kurt Binder and Dieter W. Heermann, *Monte Carlo Simulation in Statistical Physics*, 5th ed. (2010).

[23] David P. Landau and Kurt Binder, *A guide to Monte Carlo simulations in statistical physics*, 4th ed. (Cambridge Univ. Press, 2015).

[24] Sebastian Eggert and Ian Affleck, “Magnetic impurities in half-integer-spin heisenberg antiferromagnetic chains,” *Physical Review B* **46**, 10866–10883 (1992).

[25] Sebastian Eggert, “Numerical evidence for multiplicative logarithmic corrections from marginal operators,” *Physical Review B* **54**, R9612–R9615 (1996).

[26] V. Murg, J. I. Cirac, B. Pirvu, and F. Verstraete, “Matrix product operator representations,” *New Journal of Physics* **12**, 025012 (2010).

- [27] Ulrich Schollwoeck, “The density-matrix renormalization group in the age of matrix product states,” *Annals of Physics* **326**, 96–192 (2011).
- [28] Philip Richerme, Zhe-Xuan Gong, Aaron Lee, Crystal Senko, Jacob Smith, Michael Foss-Feig, Spyridon Michalakis, Alexey V. Gorshkov, and Christopher Monroe, “Non-local propagation of correlations in quantum systems with long-range interactions,” *Nature* **511**, 198–201 (2014).
- [29] P. Jurcevic, B. P. Lanyon, P. Hauke, C. Hempel, P. Zoller, R. Blatt, and C. F. Roos, “Quasiparticle engineering and entanglement propagation in a quantum many-body system,” *Nature* **511**, 202–205 (2014).
- [30] D. Porras and J. I. Cirac, “Effective quantum spin systems with trapped ions,” *Phys. Rev. Lett.* **92**, 207901 (2004).
- [31] A. Bermudez, L. Tagliacozzo, G. Sierra, and P. Richerme, “Long-range heisenberg models in quasiperiodically driven crystals of trapped ions,” *Phys. Rev. B* **95**, 024431 (2017).
- [32] B. P. Lanyon, C. Hempel, D. Nigg, M. Müller, R. Gerritsma, F. Zähringer, P. Schindler, J. T. Barreiro, M. Rambach, G. Kirchmair, and et al., “Universal digital quantum simulation with trapped ions,” *Science* **334**, 57–61 (2011).
- [33] Marin Bukov, Luca D’Alessio, and Anatoli Polkovnikov, “Universal high-frequency behavior of periodically driven systems: from dynamical stabilization to floquet engineering,” *Advances in Physics* **64**, 139–226 (2015).
- [34] Jutho Haegeman, J. Ignacio Cirac, Tobias J. Osborne, Iztok Pižorn, Henri Verschelde, and Frank Verstraete, “Time-dependent variational principle for quantum lattices,” *Physical Review Letters* **107**, 070601 (2011).
- [35] Jutho Haegeman, Christian Lubich, Ivan Oseledets, Bart Vandereycken, and Frank Verstraete, “Unifying time evolution and optimization with matrix product states,” *Physical Review B* **94**, 165116 (2016).
- [36] Bojan Žunkovič, Markus Heyl, Michael Knap, and Alessandro Silva, “Dynamical quantum phase transitions in spin chains with long-range interactions: Merging different concepts of nonequilibrium criticality,” *Phys. Rev. Lett.* **120**, 130601 (2018).
- [37] J. M. Deutsch, “Quantum statistical mechanics in a closed system,” *Phys. Rev. A* **43**, 2046–2049 (1991).
- [38] Mark Srednicki, “Chaos and quantum thermalization,” *Phys. Rev. E* **50**, 888–901 (1994).
- [39] Marcos Rigol, Vanja Dunjko, and Maxim Olshanii, “Thermalization and its mechanism for generic isolated quantum systems,” *Nature (London)* **452**, 854–858 (2008).
- [40] Christian Bartsch and Jochen Gemmer, “Dynamical typicality of quantum expectation values,” *Physical Review Letters* **102** (2009), 10.1103/PhysRevLett.102.110403.
- [41] Yasuhiro Hatsugai, “Quantized berry phases for a local characterization of spin liquids in frustrated spin systems,” *Journal of Physics: Condensed Matter* **19**, 145209 (2007).
- [42] Yasuhiro Hatsugai, “Quantized berry phases as local order parameters of quantum liquids,” *Journal of the Physical Society of Japan* **75**, 123601 (2006).
- [43] Fabian Grusdt, Norman Y. Yao, and Eugene Demler, “Topological polarons, quasiparticle invariants and their detection in 1d symmetry-protected phases,” *Physical Review B* **100**, 075126 (2019).
- [44] Fabian Grusdt, Dmitry Abanin, and Eugene Demler, “Measuring z2 topological invariants in optical lattices using interferometry,” *Physical Review A* **89**, 043621 (2014).
- [45] Marcos Atala, Monika Aidelsburger, Julio T. Barreiro, Dmitry Abanin, Takuya Kitagawa, Eugene Demler, and Immanuel Bloch, “Direct measurement of the zak phase in topological bloch bands,” *Nature Physics* **9**, 795–800 (2013).
- [46] L. Duca, T. Li, M. Reitter, I. Bloch, M. Schleier-Smith, and U. Schneider, “An aharonov-bohm interferometer for determining bloch band topology,” *Science* **347**, 288–292 (2015).
- [47] Dmitry A. Abanin, Takuya Kitagawa, Immanuel Bloch, and Eugene Demler, “Interferometric approach to measuring band topology in 2d optical lattices,” *Physical Review Letters* **110**, 165304 (2013).
- [48] Ian Affleck, Tom Kennedy, Elliott H. Lieb, and Hal Tasaki, “Rigorous results on valence-bond ground states in antiferromagnets,” *Phys. Rev. Lett.* **59**, 799–802 (1987).
- [49] Christopher Mudry, Akira Furusaki, Takahiro Morimoto, and Toshiya Hikihara, “Quantum phase transitions beyond landau-ginzburg theory in one-dimensional space revisited,” *Phys. Rev. B* **99**, 205153 (2019).
- [50] Brenden Roberts, Shenghan Jiang, and Olexei I. Motrunich, “Deconfined quantum critical point in one dimension,” *Phys. Rev. B* **99**, 165143 (2019).
- [51] Alexei Kitaev and John Preskill, “Topological entanglement entropy,” *Phys. Rev. Lett.* **96**, 110404 (2006).
- [52] J. F. Cornwell and Warren W. Buck, “Group theory in physics: An introduction,” *Physics Today* **51**, 67–68 (1998).
- [53] F. D. M. Haldane, “Nonlinear field theory of large-spin heisenberg antiferromagnets: Semiclassically quantized solitons of the one-dimensional easy-axis néel state,” *Physical Review Letters* **50**, 1153–1156 (1983).